

From *in vitro* studies to product information useful for patients: Evaluation of physical properties and the stability of nasal spray devices containing hydroxypropyl methylcellulose-based liquid and powder formulations

PEERAWAS KOPONGPANICH¹
VEERAKIET BOONKANOKWONG² 
VARIN TITAPIWATANAKUN³ 
RUTTHAPOL SRITHARADOL^{2*} 

¹ MSc. Program in Research for Enterprise, Faculty of Pharmaceutical Sciences, Chulalongkorn University Bangkok 10330, Thailand

² Department of Pharmaceutics and Industrial Pharmacy, Faculty of Pharmaceutical Sciences, Chulalongkorn University, Bangkok 10330, Thailand

³ Cyclodextrin Application and Nanotechnology-based Delivery System Research Unit, Chulalongkorn University, Bangkok 10330 Thailand

Accepted May 16, 2025
Published online May 17, 2025

ABSTRACT

Hydroxypropyl methylcellulose (HPMC)-based formulations are commonly used in nasal sprays due to their gelling and viscosity-enhancing properties. However, data on *in vitro* studies that mimic patient use remain limited. This study investigated two commercial HPMC-based aqueous formulations and HPMC-based powder formulations to provide an understanding of the relationship between the physical properties, their performance, and the stability of nasal products. Physical properties, quality tests focused on shot mass and shot volume were assessed. The coverage area within the nasal cavity was examined at various angles of actuation (15°, 30°, 45°, and 80°) using a simulated inhalation model. The 45° spray angle exhibited the highest coverage area (%) within the nasal cavity. Devices containing liquid formulations demonstrated more reproducible shot mass and shot volume compared to dry powder preparations. These findings provide valuable insights for patients and manufacturers, leading to a better understanding of optimal usage and formulation effectiveness.

Keywords: adhesive, liquid, polymer, powder, spray deposition

INTRODUCTION

Nasal sprays are pharmaceutical formulations designed to deliver drug substances directly into the nasal cavity as fine droplets or masses. These substances, available in various forms such as solutions, suspensions, and powders, are typically dispensed from non-pressurised containers equipped with metered-dose spray pumps to allow for multiple sprays. The nasal cavity, characterised by its complex geometry and specific anatomical regions, serves as an attractive route for drug delivery aimed at achieving either local or systemic effects. Understanding the regional drug deposition patterns within the nasal cavity is crucial for optimising nasal drug delivery and targeting the site of action (1).

* Correspondence; e-mail: Rutthapol.s@chula.ac.th

The COVID-19 pandemic has heightened interest in nasal spray formulations for infection prevention. Specific functional excipients like hydroxypropyl methylcellulose (HPMC) and carrageenan are incorporated in these sprays to form physical barriers in the nostrils, trapping, inactivating, and removing airborne allergens, germs, and viruses before they reach infection sites (2–4). Carrageenan, used as a gelling agent, has demonstrated *in vitro* efficacy in blocking SARS-CoV-2 and influenza infections (5–7). HPMC, widely utilised in pharmaceutical formulations for its mucoadhesive properties, produces clear aqueous solutions with minimal undissolved fibres, making it superior to methylcellulose (8). Recently, an HPMC-based nasal spray with human IgG1 antibodies was approved by the Thai FDA, showcasing its safety and efficacy against SARS-CoV-2 infections (9). Additionally, HPMC powder insufflation has shown no adverse systemic effects, indicating a favourable safety profile (10).

Typically, HPMC-based nasal sprays are marketed in solid dosage forms as dry powders (10–11). These formulations, solid or liquid, form gels upon contact with the nasal mucosa. The solid form transforms into a mucus-like gel after being sprayed into the nasal cavity and interacting with mucus, meanwhile, the gel-forming behaviour of aqueous formulations depends on their specific compositions and viscous properties of HPMC, which facilitate retention in the nasal cavity and extend the duration of attachment for gel formation (12). Besides the active substance, several factors affecting nasal sprays, such as formulation, container closure system, and manufacturing processes, must be considered to ensure effective dose delivery to patients (13).

Previous studies have investigated the efficacy and safety of HPMC-based nasal formulations. For instance, the safety of HPMC-based nasal powders has been evaluated, demonstrating their effectiveness in forming robust mucosal barriers (10). Similarly, studies have shown the virucidal activity of HPMC-based nasal sprays, highlighting their potential in preventing respiratory infections (11). Recent research has examined the nasal delivery of encapsulated recombinant ACE2 as a prophylactic treatment for SARS-CoV-2, presenting innovative approaches to nasal formulations (14). Additionally, another study provided a comprehensive overview of both *in vitro* and *in vivo* techniques used to characterise intranasal protein and peptide formulations for brain targeting, underscoring the advancements in nasal drug delivery systems (15). Despite these advancements, there remains a limited understanding of the comparative performance between liquid and powder formulations of HPMC-based nasal sprays, particularly under storage conditions, and their subsequent impact on delivery efficacy.

Therefore, this study aims to fill this gap by providing an assessment of different HPMC-based nasal sprays, comparing both liquid and solid dosage forms to understand the behavior of substances discharged from the containers. Accelerated aging storage conditions were applied to assess the impact of temperature and humidity on product performance. Various *in vitro* evaluations, including physical property characterization, performance quality tests (such as size distribution, zeta potential, dosage uniformity in terms of shot mass and volume), and mucoadhesive studies, were conducted. Additionally, an *in vitro* intranasal deposition study was performed to examine the effects of actuation parameters on regional deposition within a nasal cavity model. This approach aims to provide detailed product information that is useful for product development, healthcare providers, and patients, ensuring they receive treatments that are both effective and safe.

EXPERIMENTAL

Study products and sample preparation method

Four HPMC-based commercial nasal spray samples were included in this study such as 1 % HPMC-based mucoadhesive gel formulation, 3 % HPMC-based liquid formulation with human IgG1 anti-SARS-CoV-2 monoclonal antibodies (clones 1D1 and 3D2), 89.9 % HPMC-based powder containing citric acid, sodium citrate, benzalkonium chloride, and menthol, and 93 % HPMC-based powder which contains odor-controlled garlic and peppermint.

To prepare the simulated nasal electrolyte solution (SNES), 877 mg of NaCl, 298 mg of KCl, and 59 mg of anhydrous CaCl₂ were added to a 100 mL volumetric flask and dissolved in purified water to a final volume of 100 mL. The pH was then adjusted to 5.6 using 1 mol L⁻¹ HCl (16).

Porcine mucin was prepared at a concentration of 8 % (*m/m*) by using 0.8 g of mucin from porcine stomach (type III, bound sialic acid 0.5–1.5 %, partially purified powder, Sigma-Aldrich, Inc., Missouri, USA). SNES was added to the mucin to make a final mass of 10 g.

Determination of product characteristics

All samples were diluted with deionised water to achieve a final concentration of 0.1 % HPMC prior to testing in order to be able to compare the viscosity data between the HPMC liquid-based and powder-based formulations and to evaluate the impact of other excipients. 1 % HPMC-based mucoadhesive gel formulation was diluted with deionised water at a ratio of 1:10, by pipetting 1 mL of the sample into a 10 mL volumetric flask and adjusting the final volume. 3 % HPMC-based liquid formulation was diluted at a ratio of 1:30, by pipetting 333 μ L of the test sample into a 10 mL volumetric flask, followed by adjustment to a final volume. For 93 % HPMC-based powder, an accurate amount of 107.53 mg was weighed, corresponding to 100 mg of HPMC, and transferred to a 100 mL volumetric flask, where the sample was then diluted to the designated final volume. Similarly, 89.9 % HPMC-based powder was prepared by weighing 111.24 mg of the product, which is equivalent to 100 mg of HPMC, into a 100 mL volumetric flask for dilution.

The pH of each product was measured in triplicate using a pH meter (FiveEasy[®] FE20 Benchtop pH/ORP/Temperature Meter, METTLER TOLEDO[®], USA).

Viscosity measurements of the diluted solutions were conducted using a Brookfield Programmable DV-II+ Viscometer (Canada) equipped with a small sample adaptor (UL Adaptor) and an S00 spindle. All measurements were performed in triplicate at a speed of 20 rpm and a temperature of 25 °C.

The size distribution (*z*-average and PDI) and zeta potential of diluted solutions were determined by the dynamic light scattering (DLS) method using general purpose and auto mode analysis model (Malvern Zetasizer Nano, Malvern Panalytical Ltd., United Kingdom) (Disposable folded capillary zeta cell, medium: water; dispersant refractive index (RI): 1.33; viscosity (cP): 0.8872; equilibration time: 120 s; count rate: 100–200; material RI: 1.59; measurement position (mm):5.50; λ = 633 nm.). All tests were performed in triplicate at 25 °C.

The density of the liquid formulations (1 % HPMC-based mucoadhesive gel formulation, 3 % HPMC-based liquid formulation) was determined using a 10 mL pycnometer, with the mass of the gel measured in triplicate. The accurate volume of the pycnometer was established using distilled water, and all weighing processes were carried out at 25 °C. The density of the gel was calculated by dividing the mass of the gel formulation by the mass of distilled water.

For powder formulations, the bulk and tapped density were measured using a 10 mL graduated cylinder filled with approximately 6 g of the sample according to Chapter <616> of the United States Pharmacopoeia (USP) titled “Bulk Density of Powders”. The bulk density was determined by measuring the volume of a known mass of the powder in triplicate, and calculated by dividing the mass of the test sample by the volume measured to the nearest graduated unit.

Tapped density was obtained by mechanically tapping a graduated cylinder containing the powder sample after 10, 500, and 1250 taps. The corresponding volumes (V10, V500, and V1250) were recorded to the nearest graduated unit. If the difference between V500 and V1250 was less than or equal to 2 mL, V1250 was considered the tapped bulk volume. If the difference exceeded 2 mL, further increments of 1250 taps were performed until the difference between successive measurements was less than or equal to 2 mL. The tapped density was determined by dividing the mass of the test sample by the final tapped bulk volume.

Determination of the dosage uniformity by shot mass and shot volume

The initial mass of each sample was recorded before the first five actuations, which were used for priming the spray device. Following the priming process, the mass of the spray container was recorded. For each individual actuation, the pump spray mass was measured by fully actuating the spray, holding it for 1 second, and subsequently releasing the pump. Prior to weighing, the tip of the pump was wiped clean to ensure accuracy. The spray was continued until the container was empty, and all measurements were conducted in triplicate.

The shot mass and shot volume were calculated as averages of ten consecutive actuations taken at the beginning, middle, and end of the delivery process. Additionally, the percentage change between the initial and final measurements was computed. Shot volume was determined by applying a conversion factor based on the density. The beginning, middle, and endpoints were defined by adjusting the measurements to exclude the last 10 % of deliveries, representing the minimum fill amount. The cumulative mass of the adjusted number of deliveries was defined as the total delivery mass.

Deposition area of HPMC-based aqueous formulations

A 3D-printed nasal cast (Harn Engineering Solution PCL, in collaboration with the Faculty of Engineering, Chulalongkorn University, Thailand) was utilised in conjunction with SAR-GEL® BLUE, an indicator that changes colour from yellow to blue upon contact with water. The nasal cast can be divided along a sagittal plane into two primary components: the nasal septum and the turbinate region. The anterior portion of the cast terminates at the nostril, while the posterior portion extends to the nasopharynx. Additionally, the turbinate side can be further subdivided into two distinct parts at its midpoint. The

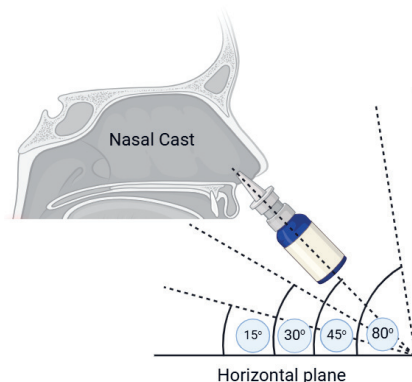


Fig. 1. Schematic of spray angle on the deposition in the nasal cast.

nasal cast was connected to a vacuum pump (GAST, DOA-P504-BN-LabModel), which provides a flow rate of approximately 0.99 cfm (28.3 L min⁻¹) to simulate inhalation conditions. To assess the full deposition area (cm²), the inner surface of the nasal model was thoroughly coated with SAR-GEL[®] BLUE, followed by the application of a fine mist of water using a fog spray bottle. Subsequently, the effect of the spray angle on the deposition of the HPMC-based aqueous formulations was evaluated at 15°, 30°, 45°, and 80° (Fig. 1). The number of actuations was performed twice for 1 % HPMC-based mucoadhesive gel formulation and once for 3 % HPMC-based liquid formulation to ensure an equivalent quantity of formulations was delivered.

For the determination of the formulation deposition area (cm²), after the nasal cast was sprayed with the HPMC-based aqueous formulations with a 1-minute latency period to allow the pre-applied SAR gel to fully transition from yellow to blue. Afterwards, the pump was turned off, and the model was then separated into the septum and turbinate sections of the nasal cavity. Each section was positioned on a black background 60 centimetres away from a camera, and images were captured in triplicate at a magnification of 2.5, with a 4:3 aspect ratio. The resulting images were imported into Adobe Photoshop CC 2019, maintaining dimensions of 1479 × 1109 pixels (totalling 102,860 pixels) at 96 dpi. Images were adjusted for brightness and contrast to enhance the colour change effect. The Quick Selection Tool was utilised to isolate the blue areas corresponding to the gel deposition. The selected area was converted from pixels to cm² using a conversion factor based on the area of a square paper. The variation in area selection was neutralised by averaging the measurements in triplicate. The total deposition area was reported as the sum of the turbinate and septum areas. The intranasal coverage area was then compared to the total deposition area and expressed as a percentage (Equation 1). To validate the area measurements in the images, white square paper samples of 1 cm², 2 cm², and 4 cm² were placed within the photographic area. Images of these square papers were subsequently imported into the software for area measurement in pixels. The measured pixel area was then calculated and compared with the actual dimensions of the square paper.

$$\text{Percentage coverage} = (\text{Intranasal coverage area} / \text{Total deposition area}) \times 100 \quad (1)$$

Assessment of mucoadhesive property

Mixed cellulose ester membranes (Merck Millipore, California, USA) were utilised to simulate intranasal tissue and maintain uniformity throughout all sample testing. This was due to that artificial membranes provide a uniform and constant surface, regulated pore size, and improved chemical and physical stability, all of which contribute to increased reproducibility and dependability of the findings. To mimic physiological conditions and simulate the intended application process, the membrane was pre-soaked in an 8 % (*m/m*) solution of porcine mucin to replicate intranasal conditions. A mixture comprising 100 μL of gel formulations and 8 mg of powder formulations was uniformly applied to the wetted membrane. This technique allows the interaction between the formulation and the moist membrane to closely resemble real-life conditions. The mucoadhesive properties were assessed using a texture analyser (TA.XT plus, Stable Micro System Ltd., United Kingdom) equipped with a 5 kg load cell and a 1-centimetre diameter cylindrical probe. The wetted membrane was securely fixed to a mucoadhesion rig (A/MUC), and a preload force of 0.2 N was applied for 30 seconds. Following the preload, the cylindrical probe was raised at a rate of 0.1 mm s^{-1} .

The mucoadhesive properties of the two formulations were quantified in terms of adhesive force (F , mN) and adhesive work (A , mN·s), with each measurement conducted in triplicate.

Determination of formulation stability under accelerated ageing conditions

A stability study of four nasal products was conducted following the ASEAN guidelines on the stability of drug products under zone IVb accelerated ageing conditions ($40 \pm 2\text{ }^\circ\text{C}$, $75 \pm 5\text{ \% RH}$) over a duration of 3 months. Following this period, the formulations were evaluated for various physical properties, including particle size distribution, zeta potential, mucoadhesive characteristics, and dosage uniformity. A comparison of these physical properties between the initial investigational phase and the storage period was performed to assess any changes.

Statistical analysis

All quantitative results were expressed as means (SD). Statistical analyses were performed using IBM SPSS[®] Statistics software version 29.0.0.0 and GraphPad Prism software version 9.0.0. The data were statistically analysed using the Shapiro-Wilk test to assess normality and Levene's test to evaluate the homogeneity of variances. For data that met the assumptions of normality and homogeneity, an Analysis of Variance (ANOVA) was conducted to determine any significant differences between groups, with a significance level at 0.05 ($p < 0.05$). For non-parametric data, group comparisons were made using the Kruskal-Wallis test, with the Bonferroni correction applied to adjust significance values for multiple comparisons.

RESULTS AND DISCUSSIONS

Physical characterization

The development of nasal spray products necessitates careful consideration of formulation and device aspects (17). Critical physical parameters of nasal spray formulations

Table I. Physical characterizations of gel and powder form of nasal spray products

Formulation	pH	Density (g mL ⁻¹) ^a	Viscosity (cP)		Initial investigational period			Storage period		
			Initial formulation	Diluted 0.1 % HPMC	Z-average (d.nm)	Size distribution	PDI	Zeta- potential (mV)	Z-average (d.nm)	Size distribution
1 % HPMC-based mucoadhesive gel formulation	3.69 (0.006)	1.01 (0.0003)	23.87 (0.06)	2.43 (0.02)	120.58 (56.53)	0.51 (0.13)	-5.27 (1.79)	177.3 (5.52)	0.63 (0.09)	0.00 (0.02)
93 % HPMC-based powder	5.51 (0.015)	0.26 (0.01) /0.44 (0.00)	NA	2.42 (0.04)	469.53 (247.41)	0.81 (0.09)	-2.48 (1.02)	410.8 (117.29)	0.63 (0.13)	-2.52 (1.98)
3 % HPMC-based liquid formulation	5.88 (0.017)	1.02 (0.0005)	21.10 (0.10)	2.02 (0.04)	89.09 (36.18)	0.85 (0.21)	-0.12 (0.14)	276.5 (13.51)	0.55 (0.11)	-0.70 (0.10)
89.9 % HPMC-based powder	3.83 (0.012)	0.11 (0.006) /0.19 (0.009)	NA	1.95 (0.01)	79.63 (63.17)	0.74 (0.14)	-1.25 (0.57)	75.74 (9.58)	0.86 (0.09)	-1.47 (0.46)

^a Density of powder formulations (93 % HPMC-based powder and 89.9 % HPMC-based powder) was shown in bulk/tapped density. Data represented in mean (SD), n = 3. HPMC – hydroxypropyl methylcellulose, PDI – polydispersity index, NA – not applicable.

including pH, osmolarity, viscosity, density, and mucoadhesive properties, significantly affect product performance, drug absorption, and bioavailability. The US FDA Chemistry, Manufacturing, and Controls (CMC) guidance suggests the measurement of pH, osmolarity, and viscosity as part of product specifications.

The physical characterisations of the nasal spray products, including pH, density, and viscosity, were presented in Table I. An optimal pH range for nasal spray formulations, to avoid nasal irritation and sneezing and to prevent microbial growth, is between 4.5 and 6.5 (18–19), which was found in the 3 % HPMC-based liquid formulation (5.88) and 93 % HPMC-based powder (5.51). Previous studies have shown that coronaviruses were effectively inactivated at pH 3.0 to 3.5. (20–22). Although the pH values of 3.69 for the 1 % HPMC-based mucoadhesive gel formulation and 3.83 for the 89.9 % HPMC-based powder formulation are slightly above the optimal range for virucidal activity against coronaviruses, their protective action on the nasal epithelium from virus particles may be attributed to other mechanisms, such as virus particle trapping. Therefore, these HPMC formulations are suited within a pH range that may facilitate viral inactivation (23).

The calculated densities of the gel formulations were 1.01 g mL⁻¹ for the 1 % HPMC-based mucoadhesive gel formulation and 1.02 g mL⁻¹ for the 3 % HPMC-based liquid formulation. The bulk and tapped densities of 93 % HPMC-based powder

der and 89.9 % HPMC-based powder were 0.26 and 0.44 g mL⁻¹, and 0.11 and 0.19 g mL⁻¹, respectively. These results indicate very poor flowability of the powders, likely due to the adhesive properties of the HPMC-based formulations (24).

Viscosity is a key factor influencing droplet size distribution and drug deposition within the nasal cavity. Previous studies on HPMC-based nasal spray formulations have shown that an increase in viscosity is associated with larger droplet sizes and reduced anterior deposition (25). Higher viscosity also enhances interactions with nasal mucus, thereby increasing mucoadhesive properties and nasal residence time (26). The combination and concentration of polymers, such as HPMC, have a concentration-dependent impact on viscosity, and comparisons can be inferred based on the concentration of HPMC (19, 27). In this study, the viscosity values for all four diluted formulations were around 2 cP, consistent with previous reports for 0.1 % HPMC nasal spray formulations (25). This consistency likely results from diluting all formulations to obtain a 0.1 % HPMC concentration in order to compare the viscosity of the powder formulation, suggesting that other excipients do not significantly impact viscosity. However, a slight difference in initial viscosity was observed for 1 % HPMC-based mucoadhesive gel formulation and 3 % HPMC-based liquid formulation, that was 23.87 and 21.10 cP, respectively.

Physical attributes such as the Z-average, PDI, and zeta potential of the formulations were characterised using dynamic light scattering (DLS). As shown in Table I, 93 % HPMC-based powder had the largest particle size distribution with a Z-average of 469.53 nm. The PDI was greater than 0.5 for all products, indicating a heterogeneous population. The zeta potential values ranged from -0.12 to -5.27 mV. Typically, particles with zeta potentials more positive than +30 mV or more negative than -30 mV are considered stable dispersion (28). However, the dispersion stability of the zeta potential value was significant to the HPMC-based aqueous formulations and does not indicate the stability of solid particles (29). In addition, a positive colloidal charge would generally be preferred since mucin molecules from mucous membranes exhibit a negative charge. They can thus interact with electrostatic interactions, leading to mucoadhesive action. However, the pure HPMC solution generally has a slightly negative charge, with the value of zeta potential of -2.14 to -3.4 mV. In this study, the mucoadhesive mechanism of formulation and mucous membrane could mainly result from gel-forming behaviour (30–32).

Determination of the dosage uniformity by shot mass and shot volume

In the characterisation of nasal sprays, the delivered dose, including shot mass and shot volume, must be considered according to the FDA Chemistry, Manufacturing, and Controls (CMC) guidance and the European Medicines Agency (EMA) guidelines. The purpose of evaluating shot mass is to ensure reproducible and precise dosing by weighing the total mass before and after each actuation.

The average number of deliveries per container for the liquid formulations was 295 ± 7 for the 1 % HPMC-based mucoadhesive gel formulation and 159 ± 3 for the 3 % HPMC-based liquid formulation. For the dry powder formulations (93 % HPMC-based powder and 89.9 % HPMC-based powder), the number of deliveries was standardised to 200 based on the product labels. After a 10 % deduction, the mean total delivery amounts were 14,555.20 ± 172.71 mg (14.11 ± 0.17 mL) for 1 % HPMC-based mucoadhesive gel formulation, 14,295.41 ± 657.93 mg (13.92 ± 0.66 mL) for 3 % HPMC-based liquid formulation, 677.27 ± 100.66 mg for 93 % HPMC-based powder, and 861.44 ± 62.31 mg for 89.9 % HPMC-based powder, as shown in Table II.

Table II. Consistency of dispensing by shot mass and shot volume

Sample	Avg. No. of deliveries	Avg. total delivery mass (mg)	Avg. total delivery volume (mL)	Initial investigational period						% Change of E to B
				Shot mass (mg)			Shot volume (µL)			
				B	M	E	B	M	E	
1 % HPMC-based mucoadhesive gel formulation	295 (7)	14555.20 (172.71)	14.11 (0.17)	55.15 (1.24) [#]	54.20 (2.08) [#]	51.50 (1.18) ^{**}	54.58 (1.22) [#]	53.64 (2.06) [#]	50.97 (1.17) ^{**}	-6.61
				9.56 (7.70) ⁺⁺	2.79 (2.12) ^{**}	1.05 (0.46) ^{**}	NA	NA	NA	NA
3 % HPMC-based liquid formulation	159 (3)	14295.41 (65793)	13.92 (0.66)	103.95 (1.86) [#]	105.88 (4.80) [#]	80.99 (36.61) ⁺⁺	101.45 (1.81) [#]	103.34 (4.69) [#]	79.05 (35.73) ⁺⁺	-22.08
				4.76 (5.25)	6.22 (7.84)	4.32 (3.43)	NA	NA	NA	NA
89.9 % HPMC-based powder	200 ^a	861.44 (62.31)	NA	4.76 (5.25)	6.22 (7.84)	4.32 (3.43)	NA	NA	NA	NA
				Stability period						
Sample	Avg. No. of deliveries	Avg. total delivery mass (mg)	Avg. total delivery volume (mL)	Stability period						% Change of E to B
				Shot mass (mg)			Shot volume (µL)			
				B	M	E	B	M	E	
1 % HPMC-based mucoadhesive gel formulation	299 (6)	14275.94 (432.86)	14.14 (0.52)	51.81 (11.1) [#]	54.26 (14.72) [#]	47.35 (6.98) ^{**}	51.30 (11.10) [#]	53.73 (3.80) [#]	46.88 (6.91) ^{**}	-8.62
				3.29 (3.92)	2.59 (1.72)	2.04 (1.10)	NA	NA	NA	NA
3 % HPMC-based liquid formulation	160 (8)	13321.03 (362.78)	13.00 (0.35)	102.09 (2.03) ⁺⁺	93.84 (6.38) ^{**}	75.21 (20.37) ^{**}	100.09 (1.99) ⁺⁺	92.00 (6.25) ^{**}	73.74 (19.98) ^{**}	-26.33
				1.32 (1.70)	2.44 (2.97)	2.22 (2.10)	NA	NA	NA	NA
89.9 % HPMC-based powder	200 ^a	476.65 (87.32)	NA	1.32 (1.70)	2.44 (2.97)	2.22 (2.10)	68.18	NA	NA	NA

^a For dry powder formulations (93 % HPMC-based powder and 89.9 % HPMC-based powder) the number of deliveries was controlled at 200 deliveries according to the products' label. ^{**} $p < 0.001$ significant difference compared to the beginning; ⁺⁺ $p < 0.001$ significant difference compared to the middle; [#] $p < 0.001$ significant difference compared to the end. Significance values have been adjusted by the Bonferroni correction for multiple tests. Data represented in mean (SD), $n = 3$. NA - not applicable.

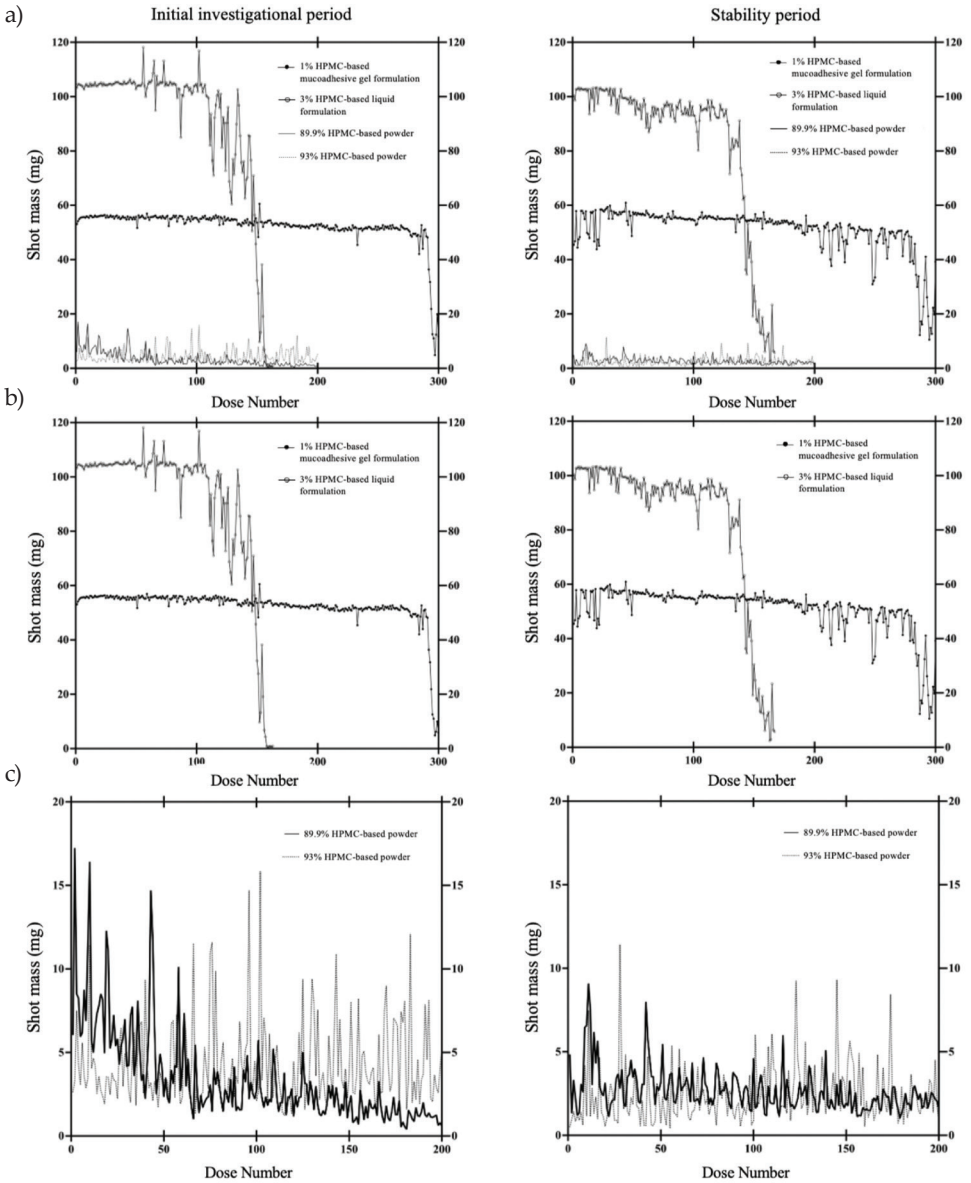


Fig. 2. Shot mass analysis compared between the initial investigational period (left) and stability period (right) of a) all formulations, b) gel and liquid formulations, and c) powder formulations.

The shot mass and shot volume of 1% HPMC-based mucoadhesive gel formulation at the end of use exhibited a significant difference to the beginning and middle deliveries

($p < 0.001$), with percent changes of the end when compared to the beginning of shot mass and shot volume -6.62 and -6.61 %, respectively. For the 3 % HPMC-based liquid formulation, the shot mass and shot volume at the end also showed significant differences compared to the middle deliveries ($p < 0.001$), with percent changes of the end to the beginning deliveries of -22.09 and -22.08 %, respectively. For the powder formulation 93 % HPMC-based powder, the shot mass at the middle and end stages showed significant differences compared to the initial deliveries ($p < 0.001$), with a percent change of -89.02 %. However, the shot mass of 89.9 % HPMC-based powder showed differences between the end and beginning deliveries ($p < 0.05$), with a percent change of -9.24 %, as shown in Table II and represented in the shot mass profile in Fig. 2.

In this study, the powder formulation (93 % HPMC-based powder and 89.9 % HPMC-based powder) showed a high variation in dosage uniformity and a significant drop in percent change when comparing the end doses with the beginning doses. Both dry powder formulations exhibited relatively higher percent changes compared to the two liquid formulations, indicating dose inconsistency throughout use. This observation suggests that the delivered doses of HPMC-based liquid nasal sprays are more reproducible and precise than those of dry powder forms, likely due to differences in the aerosol generation mechanisms between the two device types.

Although delivery devices with metering valves are engineered to ensure high dose reproducibility *via* the metering chamber and spray pump system, variability can still arise. Variations in actuation parameters and the type of container, such as a squeeze bottle, can influence the characteristics of the spray, including shot mass, leading to inconsistencies in both liquid and powder delivery devices (33). It highlights the need for patient awareness regarding the optimal use of these products and emphasises the importance of monitoring patient interactions with the devices.

Deposition area of gel formulation

The total deposition area in the nasal cavity is presented in Fig. 3. Deposition areas of liquid formulations without and with a vacuum pump are shown in Figs. 4 and 5, respectively. Although the results indicated no statistically significant differences between the groups, as presented in Fig. 6, this study identified three main factors that tend to influence the nasal deposition area: *i*) the concentration of viscosity-related ingredient in the

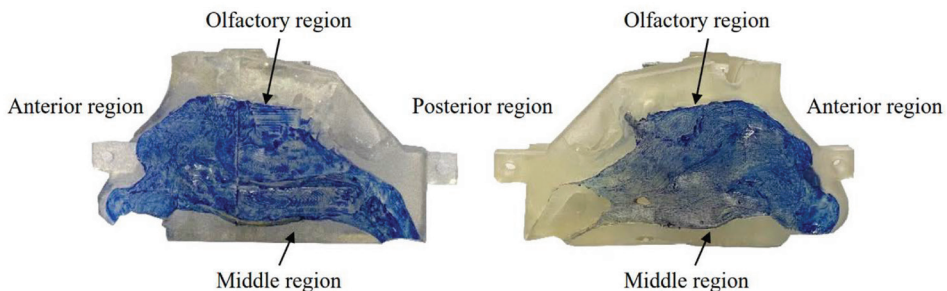


Fig. 3. Total area of the right nostril of the nasal cavity model.

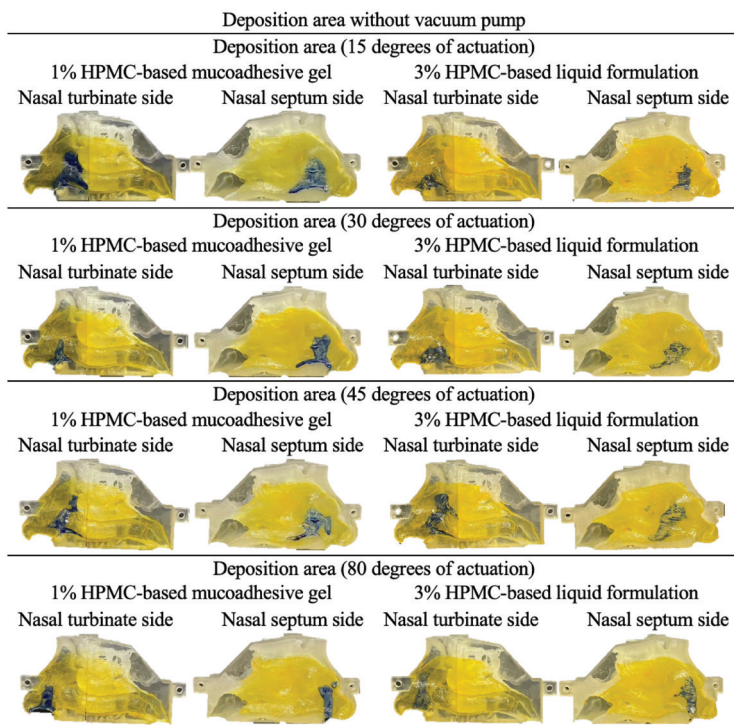


Fig. 4. Intranasal deposition of 1 % HPMC-based mucoadhesive gel and 3 % HPMC-based liquid formulation applied into the right nostril of nasal cavity model using an angle of actuation of 15, 30, 45, and 80 degrees without using vacuum pump.

product, *ii*) the spray velocity, *iii*) the presence of airflow (without a vacuum pump and using a vacuum pump), and *iv*) the spray angle (15°, 30°, 45°, and 80°) as corresponding to the previous study (34, 35).

The deposition area within the nasal cavity is a critical parameter in the performance quality testing of nasal spray products. In this study, we conclude that the formulations spread primarily due to the spray velocity. When comparing the 1 % HPMC-based mucoadhesive gel formulation to the 3 % HPMC-based liquid formulation, although there was a difference in the concentration of viscosity-related ingredient HPMC, no significant difference in deposition area was observed, likely attributable to the minimal difference in viscosity between the two formulations. Furthermore, we note that the observed differences may be due to experimental variability rather than viscosity alone.

Regarding airflow, the use of a vacuum pump showed no difference in a deposition area compared to when a vacuum pump was not used. Although the breathing profile of patients may impact the deposition areas within the nasal cavity. It has been reported that the breathing profile significantly influences nasal deposition for formulations with low viscosity about 4 cP, whereas no significant effect on nasal deposition was observed for formulations with a viscosity of 18.2 cP (36). In our study, the initial viscosity of 1 % HPMC-

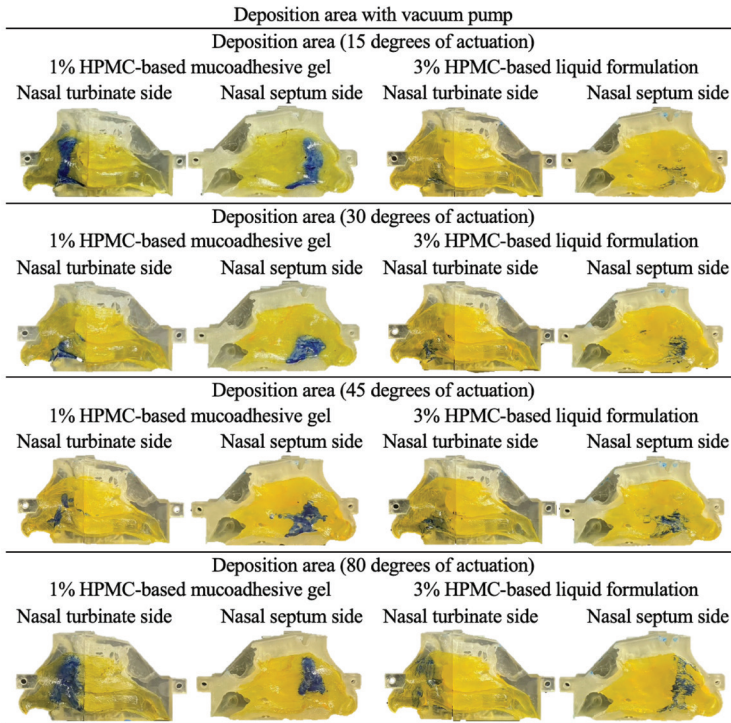


Fig. 5. Intranasal deposition of 1 % HPMC-based mucoadhesive gel and 3 % HPMC-based liquid formulation applied into the right nostril of the nasal cavity model using an angle of actuation of 15, 30, 45, and 80 degrees using a vacuum pump.

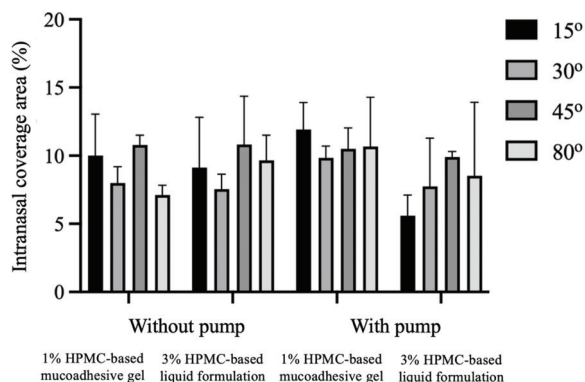


Fig. 6. Comparison of coverage area percentage of 1 % HPMC-based mucoadhesive gel and 3 % HPMC-based liquid formulation twice applied in the right nostril of the nasal cavity model using an angle of actuation of 15, 30, 45, and 80 degrees. The values are presented as mean \pm standard deviation for $n = 3$ replicates.

Table III. Summary of the mucoadhesive study

Product	Initial investigational period		Stability period	
	Peak Positive Force (mN)	Adhesive work (mN s)	Peak Positive Force (mN)	Adhesive work (mN s)
Blank (8 % mucin)	22.77 (6.25)	103.32 (10.08)	14.50 (0.69)	112.27 (8.50)
1 % HPMC-based mucoadhesive gel formulation	60.47 (14.11)	117.57 (10.33)	19.46 (1.93)	98.39 (4.62)
93 % HPMC-based powder	177.46 (19.17)	257.56 (164.89)	72.45 (14.01)	113.39 (90.64)
3 % HPMC-based liquid formulation	85.72 (14.02)	136.25 (12.95)	32.98 (13.42)	122.98 (9.51)
89.9 % HPMC-based powder	1088.16 (148.63)	771.18 (76.28)	474.68 (166.81)	673.71 (17.73)

Data represented in mean (SD), $n = 3$.

based mucoadhesive gel formulation and 3 % HPMC-based liquid formulation was 23.87 and 21.10 cP, respectively, suggesting that the breathing pattern is unlikely to affect the emitted dose and nasal deposition.

Concerning spray angles, a 45° angle exhibited the highest deposition area compared to other angles. This finding aligns with previous studies, suggesting that a 45° angle of device orientation to the nostril optimizes dose delivery to the most respiratory region (37). It is hypothesized that administering at a 45° angle enhances nasal spray deposition in the frontal sinus, which is a primary region for drug absorption (36, 38).

Mucoadhesion

Peak positive force and adhesive work are two important parameters for evaluating the effectiveness of a formulation's ability to adhere to the mucosal surface of the nasal cavity. Peak positive force refers to the maximum force recorded during the mucoadhesion test while the nasal spray is being applied or after it has come into contact with the mucosal surface. A higher peak positive force indicates stronger adhesion between the formulation and the nasal mucosa, which can lead to improved retention time in the nasal cavity. This retention time is crucial for ensuring that the drug has sufficient time for effective absorption. The viscosity of the formulation significantly influences the adhesiveness. Higher viscosity may result in a greater peak positive force due to increased interaction with the mucosa. Adhesive work, often measured in terms of energy per unit area, quantifies the energy required to separate the mucoadhesive material from the mucosal surface after adhesion. In a nasal spray formulation, high adhesive work suggests strong bonding between the formulation and the mucosa, which is desirable for drug delivery. A formulation with optimal viscosity can enhance the intimate contact with the mucosal surface and increase adhesive work, thereby improving drug retention (39).

89.9 % HPMC-based powder showed a significant difference in mucoadhesive properties compared to 8 % mucin used as a blank to serve as a physiological baseline condition and other products, as shown in Table III. Regarding mucoadhesive action, the two powder formulations exhibited relatively higher adhesive force compared to the liquid formulations. This is likely due to the higher concentrations of HPMC used as a viscosity-enhancing agent in the original formulations, with 93 % and 89.9 % HPMC-based powder, respectively. As viscosity increases, it enhances bonding with the nasal mucosa, indicating a higher mucoadhesive action (40).

The viscosity of the formulations has shown a direct relationship to the mucoadhesive effect, enabling the prediction of trends in drug absorption, bioavailability, and the residence time of the drug at the target site for specific formulation or device applications. It should be noted that electrostatic interactions are another critical factor contributing to enhanced mucoadhesive properties (39). However, in this study, zeta potential did not affect mucoadhesive measurements due to the lack of electrostatic interactions with the nasal mucosa.

Determination of formulation stability under accelerated ageing conditions

The physical stability of the four nasal products was evaluated under accelerated ageing conditions (40 ± 2 °C/ 75 ± 5 % RH for 3 months). Both liquid formulations showed a significant increase in particle size distribution, whereas particle size distribution decreased in both powder products. Specifically, the Z-average for 3 % HPMC-based liquid formulation increased nearly threefold, from 89.09 nm to 276.5 nm, whereas 89.9 % HPMC-based powder exhibited a slight decline in Z-average, from 79.63 nm to 75.74 nm, as shown in Table I. This suggests that particle agglomeration or fusion in liquid formulations may occur due to exposure to temperature and humidity changes, emphasising the importance of proper storage conditions for patients (41). In contrast, the dry powder forms appeared more stable, likely due to the absence of particle aggregation (42).

Table I shows that all formulations remained heterogeneous, with PDI values exceeding 0.5. Noticeable increases in PDI were observed for 1 % HPMC-based mucoadhesive gel formulation, 3 % HPMC-based liquid formulation, and 89.9 % HPMC-based powder, with values rising to 0.63, 0.63, and 0.86, respectively. However, a decrease in the PDI was observed for the 93 % HPMC-based powder, dropping from 0.81 to 0.63, indicating a reduction in particle size heterogeneity. A possible explanation may be attributed to sample ageing of the formulation during storage, where larger aggregates break down, resulting in a more uniform size distribution. Throughout the storage period, the zeta potential values did not change significantly, maintaining a slightly negative to neutral charge.

The shot mass profile for all nasal products remained consistent across accelerated aging conditions, as shown in Fig. 2. This data indicates good stability regarding delivered dose uniformity.

Stability data showed the same pattern as the initial investigational findings, with both positive force and positive area decreasing over time. The 89.9 % HPMC-based powder demonstrated the highest positive force and positive area, although the positive force dropped significantly from 1088.16 to 474.68 mN. A positive force of 93 % HPMC-based powder reduced from 177.46 to 72.45 mN. The 1 % HPMC-based mucoadhesive gel formulation and 3 % HPMC-based liquid formulation also showed decreases in positive force and

positive area. Increased positive forces were detected in powder formulations relative to their liquid formulation, which can be attributed to the higher content of HPMC and the resulting increase in viscosity. In contrast, accelerated ageing conditions may impact the stability of the formulation, resulting in a decrease in the mucoadhesive properties of degraded HPMC and a corresponding reduction in viscosity (39, 43). Despite these variations, the pH of the formulations remained within the acceptable range. Thus, the storage conditions play a critical role as they significantly influence the physical stability of the products.

CONCLUSIONS

This study elucidates the relationship between the physical properties and performance of HPMC-based nasal sprays, providing valuable information on optimal use and storage practices for both patients and manufacturers. Uniformity of dosage forms, typically overlooked in product registrations, was considered in this research. Various factors, including formulations, devices, storage conditions, and administration techniques, influenced drug deposition. Specifically, accelerated ageing conditions impacted the properties of HPMC in the test samples, underscoring the recommendation to avoid exposure to moisture and high temperatures to maintain product integrity. Healthcare professionals should also consider potential dose adjustments for devices using dry powder formulations, as these may not deliver uniform doses. Furthermore, proper administration techniques, such as delivering at a 45° angle, should be communicated to patients to maximise the performance of the delivery device and treatment efficacy. Despite these findings, further study is necessary to address data gaps and enhance the understanding of the critical parameters involved in the development and quality testing of nasal sprays.

Supplementary material is available upon request.

Acknowledgements. – This research was supported by Procter & Gamble Trading (Thailand) Ltd. throughout the research process.

Conflicts of interest. – The authors declare no conflict of interest.

Funding. – This research was funded by Procter & Gamble Trading (Thailand) Ltd.

Authors contributions. – Conceptualization, V.B., V.T. and R.S.; methodology, P.K.; analysis P.K.; investigation, P.K.; writing, original draft preparation, R.S.; writing, review and editing, V.B., V.T. and R.S.; supervision, R.S. All authors have read and agreed to the published version of the manuscript.

REFERENCES

1. S. Le Guellec, S. Ehrmann and L. Vecellio, *In vitro – in vivo* correlation of intranasal drug deposition, *Adv. Drug Deliv. Rev.* **170** (2021) 340–352; <https://doi.org/10.1016/j.addr.2020.09.002>
2. K. Bentley and R. Stanton, Hydroxypropyl methylcellulose-based nasal sprays effectively inhibit *in vitro* SARS-CoV-2 infection and spread, *Viruses* **13**(12) (2021) Article ID 2345 (10 pages); <https://doi.org/10.3390/v13122345>
3. D. Schütz, C. Conzelmann, G. Fois, R. Groß, T. Weil, L. Wettstein, S. Stenger, A. Zelikin, T. K. Hoffmann, M. Frick, J. A. Müller and J. Münch, Carrageenan-containing over-the-counter nasal and oral sprays inhibit SARS-CoV-2 infection of airway epithelial cultures, *Am. J. Physiol. Lung Cell Mol. Physiol.* **320**(5) (2021) 750–766; <https://doi.org/10.1152/ajplung.00552.2020>

4. D. Hull, P. Rennie, A. Noronha, C. Poore, N. Harrington, V. Fearnley and D. Passali, Effects of creating a non-specific, virus-hostile environment in the nasopharynx on symptoms and duration of common cold, *Acta Otorhinolaryngol. Ital.* 27(2) (2007) 73–77.
5. M. Morokutti-Kurz, M. Fröba, P. Graf, M. Große, A. Grassauer, J. Auth, U. Schubert and E. Prieschl-Grassauer, Iota-carrageenan neutralizes SARS-CoV-2 and inhibits viral replication *in vitro*, *PLoS One* 16(2) (2021) e0237480 (13 pages); <https://doi.org/10.1371/journal.pone.0237480>
6. Y. Jang, H. Shin, M. K. Lee, O. S. Kwon, J. S. Shin, Y. I. Kim, C. W. Kim, H. R. Lee and M. Kim, Antiviral activity of lambda-carrageenan against influenza viruses and severe acute respiratory syndrome coronavirus 2, *Sci. Rep.* 11(1) (2021) Article ID 821 (12 pages); <https://doi.org/10.1038/s41598-020-80896-9>
7. A. Leibbrandt, C. Meier, M. König-Schuster, R. Weinmüllner, D. Kalthoff, B. Pflugfelder, P. Graf, B. Frank-Gehrke, M. Beer, T. Fazekas, H. Unger, E. Prieschl-Grassauer and A. Grassauer, Iota-carrageenan is a potent inhibitor of influenza A virus infection, *PLoS One* 5(12) (2010) e14320 (11 pages); <https://doi.org/10.1371/journal.pone.0014320>
8. A. J. Hickey and S. R. da Rocha, *Pharmaceutical Inhalation Aerosol Technology*, CRC Press, Boca Raton 2019; <https://doi.org/10.1201/9780429055201>
9. T. Imsuwansri, T. Jongthitnon, N. Pojdoung, N. Meesiripan, S. Sakarin, C. Boonkrai, T. Wongtangprasert, T. Phakham, T. Audomsun, C. Attakitbanha, P. Saelao, P. Muanwien, M. T. Tian, S. Tongchusak, B. Sangruji, D. L. Wannigama, C. Sawangmake, W. Rodprasert, Q. D. Le, S. D. Purbantor, K. Vasuntrarak, S. Nantavisai, S. Sirilak, B. Uppapong, S. Sapsutthipas, S. Trisiriwanich, T. Somporn, A. Usoo, N. Mingngamsup, S. Phumiamorn, P. Aumklad, K. Arunprasert, P. Patrojanasophon, P. Opanasopit, N. Pesirikan, L. Nitisaporn, J. Pitchayakorn, T. Narkthong, B. Mahong, K. Chaiyo, K. Srisutthisamphan, R. Viriyakitkosol, S. Aeumjaturapat, A. Jongkaewwattana, S. Bunnag and T. Pisitkun, Assessment of safety and intranasal neutralizing antibodies of HPMC-based human anti-SARS-CoV-2 IgG1 nasal spray in healthy volunteers, *Sci. Rep.* 13 (2023) Article ID 15648 (12 pages); <https://doi.org/10.1038/s41598-023-42539-7>
10. T. A. Popov, J. Emberlin, P. Josling and A. Seifalian, In vitro and in vivo evaluation of the efficacy and safety of powder hydroxypropylmethylcellulose as nasal mucosal barrier, *Med. Devices* 13 (2020) 107–113; <https://doi.org/10.2147%2FMDER.S236104>
11. N. Hunt, L. Suleman, P. D. Josling and T. A. Popov, Virucidal activity of Nasaleze® Cold & Flu Blocker and Nasaleze® Travel in cell cultures infected with human pathogenic coronavirus 229-E, *bioRxiv* 23 (2021) (16 pages); <https://doi.org/10.1101/2021.09.23.461483>
12. S. Perez-Robles, C. Carotenuto and M. Minale, HPMC hydrogel formation mechanisms unveiled by the evaluation of the activation energy, *Polymers* 14(3) (2022) Article ID 635 (10 pages); <https://doi.org/10.3390/polym14030635>
13. U.S. Department of Health and Human Services FaDA, Center for Drug Evaluation and Research (CDER) (2002) Guidance for Industry: Nasal Spray and Inhalation Solution, Suspension, and Spray Drug Products – Chemistry, Manufacturing, and Controls Documentation
14. A. Baldelli, C. Y. J. Wong, H. Oguzlu, H. Gholizadeh, Y. Guo, H. X. Ong, A. Singh, D. Traini and A. Pratap-Singh, Nasal delivery of encapsulated recombinant ACE2 as a prophylactic drug for SARS-CoV-2, *Int. J. Pharm.* 655 (2024) Article ID 124009 (13 pages); <https://doi.org/10.1016/j.ijpharm.2024.124009>
15. C. Y. J. Wong, A. Baldelli, O. Tietz, J. van der Hoven, J. Suman, H. X. Ong and D. Traini, An overview of in vitro and in vivo techniques for characterization of intranasal protein and peptide formulations for brain targeting, *Int. J. Pharm.* 654 (2024) Article ID 123922 (12 pages); <https://doi.org/10.1016/j.ijpharm.2024.123922>
16. B. Sipos, I. Csóka, N. Szivacszi, M. Budai-Szűcs, Z. Schelcz, I. Zupkó, P. Szabó-Révész, B. Volk and G. Katona, Mucoadhesive meloxicam-loaded nanoemulsions: Development, characterization and

- nasal applicability studies, *Eur. J. Pharm. Sci.* **175** (2022) Article ID 106229 (10 pages); <https://doi.org/10.1016/j.ejps.2022.106229>
17. S. Trows, K. Wuchner, R. Spycher and H. Steckel, Analytical challenges and regulatory requirements for nasal drug products in Europe and the U.S., *Pharmaceutics* **6**(2) (2014) 195–219; <https://doi.org/10.3390/pharmaceutics6020195>
 18. F. Laffleur and B. Bauer, Progress in nasal drug delivery systems, *Int. J. Pharm.* **607** (2021) Article ID 120994; <https://doi.org/10.1016/j.ijpharm.2021.120994>
 19. Y. Shin, R. Kokate, V. Desai, A. Bhushan and G. Kaushal, D-cycloserine nasal formulation development for anxiety disorders by using polymeric gels, *JDDT* **12** (2018) 142–153; <https://doi.org/10.5582/ddt.2018.01017>
 20. P. Rennie, P. Bowtell, D. Hull, D. Charbonneau, R. Lambkin-Williams and J. Oxford, Low pH gel intranasal sprays inactivate influenza viruses *in vitro* and protect ferrets against influenza infection, *Respir. Res.* **8** (2007) Article ID 38 (7 pages); <https://doi.org/10.1186/1465-9921-8-38>
 21. M. E. Darnell, K. Subbarao, S. M. Feinstone and D. R. Taylor, Inactivation of the coronavirus that induces severe acute respiratory syndrome, SARS-CoV, *J. Virol. Methods* **121** (2004) 85–89; <https://doi.org/10.1016/j.jviromet.2004.06.006>
 22. K. Shmuel, M. Dalia, L. Tair and N. Yaakov, Low pH Hypromellose (Taffix) nasal powder spray could reduce SARS-CoV-2 infection rate post mass-gathering event at a highly endemic community: An observational prospective open label user survey, *Expert. Rev. Anti. Infect. Ther.* **19**(10) (2021) 1325–1330; <https://doi.org/10.1080/14787210.2021.1908127>
 23. T. L. Meister, D. Todt, Y. Brüggemann, J. Steinmann, S. Banava, F. H. H. Brill, J. Steinmann, S. Pfaender and E. Steinmann, Virucidal activity of nasal sprays against severe acute respiratory syndrome coronavirus-2, *J. Hosp. Infect.* **120** (2022) 9–13; <https://doi.org/10.1016/j.jhin.2021.10.019>
 24. A. Santomaso, P. Lazzaro and P. Canu, Powder flowability and density ratios: The impact of granules packing, *Chem. Eng. Sci.* **58**(13) (2003) 2857–2874; [https://doi.org/10.1016/S0009-2509\(03\)00137-4](https://doi.org/10.1016/S0009-2509(03)00137-4)
 25. Y. Pu, A. Goodey, X. Fang and K. Jacob, A comparison of the deposition patterns of different nasal spray formulations using a nasal cast, *Aerosol. Sci. Technol.* **48** (2014) 930–938; <https://doi.org/10.1080/02786826.2014.931566>
 26. R. J. A. Moakes, S. P. Davies, Z. Stamataki and L. M. Grover, Formulation of a composite nasal spray enabling enhanced surface coverage and prophylaxis of SARS-COV-2, *Adv. Mater.* **33**(26) (2021) Article ID 2008304 (11 pages); <https://doi.org/10.1002/adma.202008304>
 27. P. Yimsiri and M. Mackley, Spin and dip coating of light-emitting polymer solutions: Matching experiment with modelling, *Chem. Eng. Sci.* **61** (2006) 3496–505; <https://doi.org/10.1016/j.ces.2005.12.018>
 28. A. Ghauri, I. Ghauri, A. M. A. Elhissi and W. Ahmed, *Advances in Medical and Surgical Engineering*, University of Central Lancashire, UK, Preston 2020.
 29. C. M. Muntu, C. Avanti, H. Hayun and S. Surini, Stability study of spray freeze-dried insulin dry powder formulations used for nose-to-brain delivery, *J. Appl. Pharm. Sci.* **10**(13) (2023) 225–237; <https://doi.org/10.7324/JAPS.2023.148983>
 30. R. Popescu, M. V. Ghica, C. E. Dinu-Pirvu, V. Anuta, D. Lupuleasa and L. Popa, New opportunity to formulate intranasal vaccines and drug delivery systems based on chitosan, *Int. J. Mol. Sci.* **21**(14) (2020) Article ID 5016 (23 pages); <https://doi.org/10.3390/ijms21145016>
 31. A. G. Beule, Physiology and pathophysiology of respiratory mucosa of the nose and the paranasal sinuses, *GMS Curr. Top. Otorhinolaryngol. Head Neck Surg.* **9** (2010) Article ID 7 (24 pages); <https://doi.org/10.3205/cto000071>
 32. R. Ghadermazi, S. Hamdipour, K. Sadeghi, R. Ghadermazi and A. Khosrowshahi Asl, Effect of various additives on the properties of the films and coatings derived from hydroxypropyl methylcellulose – A review, *Food. Sci. Nutr.* **13**(7) (2019) 3363–3377; <https://doi.org/10.1002/fsn3.1206>

33. T. R. Sosnowski, P. Rapiejko, J. Sova and K. Dobrowolska, Impact of physicochemical properties of nasal spray products on drug deposition and transport in the pediatric nasal cavity model, *Int. J. Pharm.* **574** (2020) Article ID 118911; <https://doi.org/10.1016/j.ijpharm.2019.118911>
34. S. Fang, X. Rui, Y. Zhang, Z. Yang and W. Wang, Comparative study of nasal cavity drug delivery efficiency with different nozzles in a 3D printed model, *PeerJ.* **12** (2024) e17227 (17 pages); <https://doi.org/10.7717/peerj.17227>
35. Y. Pu, A. P. Goodey, X. Fang and K. Jacob, A comparison of the deposition patterns of different nasal spray formulations using a nasal cast, *AS&T* **48**(9) (2014) 930–938; <https://doi.org/10.1080/02786826.2014.931566>
36. M. Gao, X. Shen and S. Mao, Factors influencing drug deposition in the nasal cavity upon delivery via nasal sprays, *J. Pharm. Investig.* **50**(3) (2020) 251–259; <https://doi.org/10.1007/s40005-020-00482-z>
37. X. A. Si, M. Sami and J. Xi, Liquid film translocation significantly enhances nasal spray delivery to olfactory region: A numerical simulation study, *Pharmaceutics* **13**(6) (2021) Article ID 903 (19 pages); <https://doi.org/10.3390/pharmaceutics13060903>
38. J. Siu, J. van Strien, R. Campbell, P. Roberts, M. D. Tingle, K. Inthavong and R. G. Douglas, Comparison of sinus deposition from an aqueous nasal spray and pressurised MDI in a post-endoscopic sinus surgery nasal replica, *Pharm. Res.* **39**(2) (2022) 317–327; <https://doi.org/10.1007/s11095-021-03129-2>
39. Q. Zhang, X. Li and B. R. Jasti, Role of physicochemical properties of some grades of hydroxypropyl methylcellulose on *in vitro* mucoadhesion, *Int. J. Pharm.* **609** (2021) Article ID 121218; <https://doi.org/10.1016/j.ijpharm.2021.121218>
40. A. Utkarshini, F. Tiam and U. A. Remigius, *Recent Advances in Novel Drug Carrier Systems*, IntechOpen, Rijeka 2012; <https://doi.org/10.5772/2889>
41. J. Ehrick, S. Shah, C. Shaw, V. Kulkarni, I. Coowanitwong, S. De and J. Suman, Sterile product development, formulation, Process, Quality and Regulatory Considerations *AAPS Press* **6** (2013) 99–144.
42. P. G. Djupesland, Nasal drug delivery devices: characteristics and performance in a clinical perspective – A review, *Drug Deliv. Transl. Res.* **3** (2013) 42–62; <https://doi.org/10.1007/s13346-012-0108-9>
43. Y. Qin, J. Ye, P. Ohno, T. Nah and S. Martin, Temperature-dependent viscosity of organic materials characterized by atomic force microscope, *Atmosphere* **12**(11) (2021) Article ID 1476 (10 pages); <https://doi.org/10.3390/atmos12111476>